Indian Journal of Pure & Applied Physics
Vol. 55, August 2017, pp. 574-582

A study of acoustical parameters of cupric oxide nanoparticles dispersed in aqueous solutions of various glycols

Mukesh Kumar, Neha Sawhney, Amit Kumar Sharma & Meena Sharma*
Department of Chemistry, University of Jammu, Jammu 180 006, India

Received 15 July 2016; accepted 27 February 2017

In this study cupric oxide (CuO) nanoparticles have been synthesised by precipitation method using cupric acetate dihydrate [$Cu(CH_3COO)_2.2H_2O$] as a starting material. The synthesised nanoparticles have been characterised by X-ray diffraction (XRD), transmission electron microscopy (TEM), scanning electron microscopy (SEM) and energy dispersive X-ray spectroscopy (EDX). These nanoparticles have been dispersed in three different base fluids which are 10% aqueous solutions of ethylene glycol (EG), propylene glycol (PG) and hexylene glycol (HG). Ultrasonic velocity (U), density (ρ) and viscosity (η) of these nanofluids have been measured at different concentrations of CuO nanoparticles as a function of temperatures (T = 303.15 K, 308.15 K and 313.15 K). Using these values various acoustical parameters such as adiabatic compressibility, intermolecular free length, relaxation time, acoustic impedance and attenuation coefficient have been evaluated.

Keywords: CuO nanoparticles, Ultrasonic velocity, Acoustical parameters

1 Introduction

Nanofluid is a new dimensional thermo fluid term emerged after the pioneering work by Choi[1]. Nanofluid is a solid–liquid mixture which consists of nanoparticles and a base liquid. Nanofluids have superior properties like high thermal conductivity, minimal clogging in flow passages, long-term stability, and homogeneity because of small size and large surface area of nanoparticles[2]. The nanofluids can be prepared by dispersing a very small amount of nanoparticles in the base fluid like water, ethylene glycol, propylene glycol, polyvinyl alcohol, polyvinyl pyrrolidone, etc. Using the ultrasonication the dispersion of the nanoparticles in the base fluid is made uniform. The oxide of transition metals is an important class of semiconductors having applications in electronics, catalysis and solar energy transformation[3,4]. Among the oxides of transition metals, CuO nanoparticles are of special interest because of their wide use in catalysis, metallurgy, high temperature superconductors and as efficient nanofluid in heat transfer applications[5-7]. CuO being a ceramic semi-conductive *p*-type material with a low band gap of 1.21-1.51 eV possesses wide applications in pigment and electronic device fabrication[8]. CuO nanoparticles are used for glucose sensing in blood serum[9,10]. There has been a lot of research done about nanofluids recently but most of them are related with the heat transfer properties having different contents including heat transfer enhancement[11–13], thermal conductivity measurement[14–16], thermal conductivity of suspensions[17–19], thermal properties enhancement[20], thermal transport[21], thermal conductivity improvement[22] and estimation of thermal conductivity[23], etc. Recently some new issues have been introduced in literatures like thermal diffusion coefficient of nanofluid[24], slip mechanisms in nanofluids[25], electrical conductivity of nanofluids[26], nanofluids for cooling of electronic devices[27]. Close examination of the literature indicates that only some authors studied the ultrasonic properties of nanofluids[28,29]. Despite recent advances, much more works involving theoretical, experimental and numerical research are necessary to solve the mysteries of nanofluids.

This paper is devoted to the systematic experimental study on the response of nanofluids to the ultrasonic wave propagation for the basic understanding of how the nanoparticles behave in fluids and how they interact with each other and with fluid. The main concern is to prepare homogeneous nanofluids and attaining a deeper understanding of particle-fluid and particle-particle interactions as a function of concentration and temperature.

*Corresponding author (E-mail: mlakhanpal123@gmail.com)

2 Experimental Details

2.1 Materials

The starting materials for the preparation of CuO nanoparticles were [$Cu(CH_3COO)_2.2H_2O$], CH_3COOH, NaOH, CH_3COCH_3 and C_2H_5OH. Ethylene glycol, propylene glycol and hexylene glycol were used as base fluids for the preparation of nanofluids. All the chemicals were procured from Sigma Aldrich and used without any further purification. Triply distilled water was used for the preparation of nanofluids.

2.2 Preparation of nanofluids

CuO nanoparticles were synthesized in an alkaline medium by using [$Cu(CH_3COO)_2.2H_2O$] as a precipitating agent[30]. The copper salt solution used was freshly prepared 0.2M [Cu $(CH_3COO)_2$. $2H_2O$]. The salt solution was mixed with 1 mL glacial acetic acid and the resulting solution was heated on a magnetic stirrer up to a temperature of 60 °C. Glacial acetic acid was used to prevent the hydrolysis of the copper acetate solution. On the above solution NaOH pellets were added until a pH of 10.5 where black precipitates of CuO were formed instantly. At the same pH and temperature the solution was kept at a digestion time of 30 min. After cooling to room temperature, particles were separated from the dispersion. The particles were washed many times with water, ethanol and acetone. They were separated from dispersion by centrifugation and dried at room temperature in an inert atmosphere. To obtain nanofluids of different concentrations the nanoparticles of CuO thus obtained were dispersed in three different base fluids which were 10% aqueous solutions of EG, PG and HG in various concentrations. Ultrasonic wave of frequency 4 MHz was passed through the fluid for 3 h with the help of ultrasonicator to achieve uniform dispersion of the particles.

3 Characterizations

Bruker AXS D8 Advance X-ray diffractometer was used to obtain X-ray diffraction patterns of the samples in the present study. JEOL JEM-2100 LaB6 was used for TEM studies. To examine the morphology of the synthesized nanoparticles, SEM analysis was carried out on the JEOL JSM-6390LV SEM fitted with secondary electron detector, and equipped with an attachment for the energy dispersive X-ray spectroscopy (EDX) to enable elemental composition analysis.

3.1 Measurement of ultrasonic velocity, viscosity and density

An ultrasonic interferometer provided by Mittal enterprises, New Delhi was used to measure ultrasonic velocity of nanofluids. Ultrasonic velocity was measured at a frequency of 5 MHz. Viscosity was measured by using Ostwald's viscometer. The density of various nanofluids was measured with Anton Paar DSA 5000 M, Austria. All these measurements were performed for the nanofluids of different concentrations at three different temperatures 303.15 *K*, 308.15 K and 313.15 K.

3.2 Evaluation of acoustical parameters

The acoustical parameters: adiabatic compressibility (β_{ad}), intermolecular free length (L_f), relaxation time (τ), acoustic impedance (Z) and attenuation coefficient (α/f^2) were evaluated for various nanofluids at three different temperatures using measured values of ultrasonic velocity, density and viscosity by using the following standard relations[31-34]:

$$\beta_{ad} = 1/U^2\rho \quad \ldots (1)$$

$$L_f = K_T\, \beta_{ad}^{1/2} \quad \ldots (2)$$

$$\tau = (4/3)\, \beta_{ad}\, \eta \quad \ldots (3)$$

$$Z = U \times \rho \quad \ldots (4)$$

$$\alpha/f^2 = 4\pi^2\tau/2U \quad \ldots (5)$$

where K_T is Jacobson's constant.

4 Results and Discussion

The synthesised nanoparticles were characterized by XRD, TEM, SEM and EDX. The XRD pattern of synthesised nanoparticles is depicted in Fig. 1.

The average crystallite size was determined by using Debye-Scherrer equation:

$$D = K\lambda/\beta \cos\theta \quad \ldots (6)$$

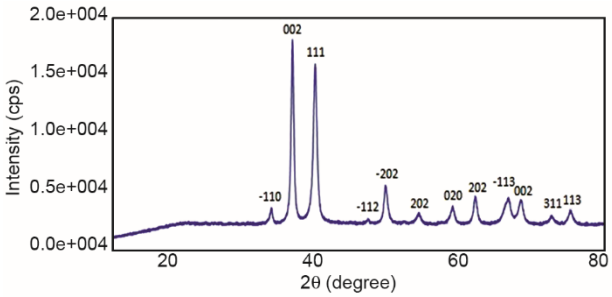

Fig. 1 – XRD pattern of CuO nanoparticles.

where K is shape factor (0.89), λ is the wavelength of the X-ray (1.54 Å) and β is the peak broadening at half the maximum intensity (FWHM) in radians and θ is the Bragg's angle.

All diffraction peaks can be indexed as the monoclinic crystal structure of CuO (space group C2/c) by comparison with data from JCPDS File No. 48-1548 with lattice constants a = 4.6837 Å, b = 3.4226 Å, c = 5.1288 Å and $\alpha = 90°$, $\beta = 99.54°$, $\gamma = 90°$ and no characteristic peaks of any other impurity were observed. The sharp peaks indicate that the product was well crystallized. The crystallite size corresponding to most intense peak was found to be 14.692 nm corresponding to 2θ value of 38.7832 and *hkl* (111).

TEM micrograph of the synthesised nanoparticles is depicted in Fig. 2. Average diameter of the nanoparticles was 15-20 nm evaluated by ImageJ software.

SEM was used to obtain the morphology of synthesized nanoparticles. SEM image clearly shows the flower like structures of nanoparticles. The stoichiometry of sample was examined by EDX spectrum. Only Cu and O signals have been detected, suggesting that the nanoparticles were only made up of Cu and O. SEM and EDX of the synthesised nanoparticles are depicted in Figs 3 and 4, respectively.

It is apprehended from Table 1 that ultrasonic velocity increases with increase in concentration of nanofluids up to 0.04 wt% and after that it starts decreasing. Thus there are structural changes occurring in the liquid system. The increase in velocity may be due to surface effects that arises out of hydrogen bonding of CuO nanoparticles with water molecules as well as with glycol molecules (CuO--water and CuO--glycol) but after 0.04 wt% ultrasonic velocity decreases which may be due to increasing inter particle interactions (CuO--CuO) which decreases CuO--water and CuO--glycol interactions. The density and viscosity followed the general liquid behaviour and showed an increase with increase in concentration. The increase in density and viscosity with increase in concentration of CuO nanoparticles may be due to some structure making tendency of the CuO nanoparticles as a result of this there is contraction in volume and hence density and viscosity showed an increasing trend.

With rise in temperature ultrasonic velocity showed an increasing trend while viscosity and density showed a decreasing trend as shown in Tables 1 and 2. Adiabatic compressibility has been

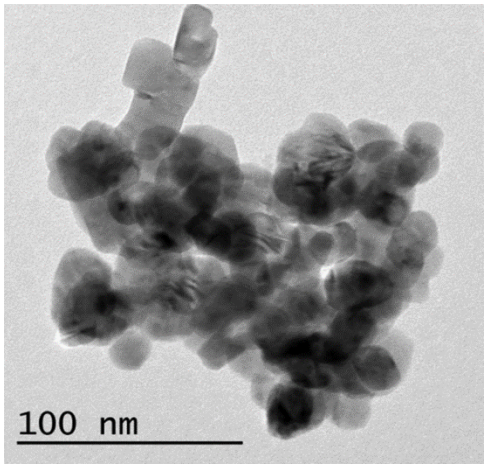

Fig. 2 – TEM micrograph of CuO nanoparticles.

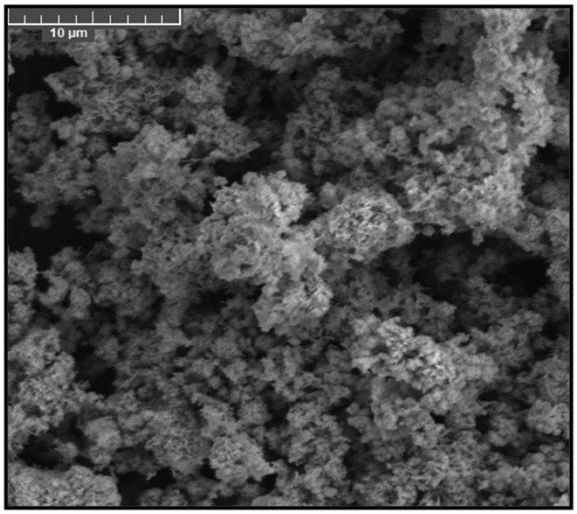

Fig. 3 – SEM micrograph of CuO nanoparticles.

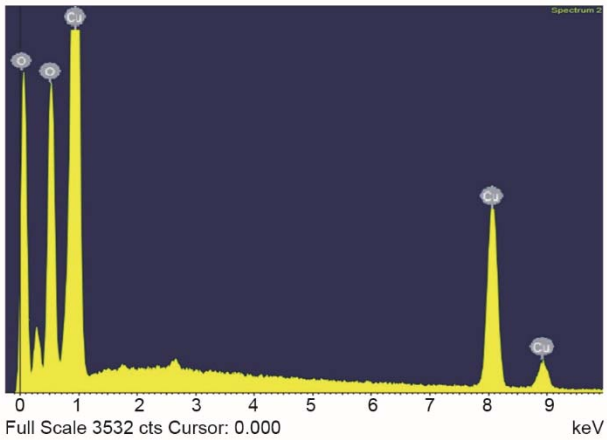

Fig. 4 – EDX spectrum of CuO nanoparticles.

Table 1 – Ultrasonic velocity and density of CuO nanofluids at three different temperatures

Concentration (wt%)	$U \times 10^{-3}$ (m s^{-1})			$\rho \times 10^{-3}$ (kg m^3)		
	EG+H_2O	PG+H_2O	HG+H_2O	EG+H_2O	PG+H_2O	HG+H_2O
			303.15 K			
0.00	1.54909	1.56450	1.56636	1.00911	1.00258	0.99504
0.02	1.55145	1.56597	1.56727	1.00956	1.00284	0.99522
0.04	1.55373	1.56733	1.56809	1.00991	1.00309	0.99539
0.06	1.55138	1.56606	1.56722	1.01015	1.00324	0.99551
0.08	1.54918	1.56483	1.56645	1.01043	1.00344	0.99565
0.10	1.54752	1.56391	1.56581	1.01076	1.00369	0.99582
			308.15 K			
0.00	1.55528	1.56820	1.57364	1.00726	1.00076	0.99320
0.02	1.55736	1.56955	1.57452	1.00770	1.00099	0.99335
0.04	1.55989	1.57093	1.57543	1.00804	1.00120	0.99349
0.06	1.55796	1.56974	1.57465	1.00831	1.00137	0.99364
0.08	1.55582	1.56855	1.57389	1.00859	1.00158	0.99379
0.10	1.55437	1.56762	1.57323	1.00891	1.00183	0.99396
			313.15 K			
0	1.56382	1.57180	1.58091	1.00523	0.99895	0.99116
0.02	1.56382	1.57307	1.58171	1.00568	0.99895	0.99131
0.04	1.56592	1.57425	1.58250	1.00601	0.99915	0.99146
0.06	1.56366	1.57299	1.58176	1.00628	0.99934	0.99161
0.08	1.56178	1.57175	1.58091	1.00656	0.99954	0.99176
0.10	1.56033	1.57093	1.58036	1.00686	0.99979	0.99193

Table 2 – Viscosity and adiabatic compressibility of CuO nanofluids at three different temperatures

Concentration (wt%)	$\eta \times 10^3$ (kg m^{-1} s^{-1})			$\beta_{ad} \times 10^{10}$ (m kg^{-1} s)		
	EG+H_2O	PG+H_2O	HG+H_2O	EG+H_2O	PG+H_2O	HG+H_2O
			303.15 K			
0.00	1.14316	1.14277	1.09244	4.12960	4.07502	4.09615
0.02	1.17486	1.17167	1.11909	4.11521	4.06632	4.09066
0.04	1.20575	1.19986	1.14542	4.10172	4.05825	4.08568
0.06	1.23585	1.22728	1.17214	4.11318	4.06423	4.08973
0.08	1.26319	1.25125	1.19325	4.12373	4.06981	4.09317
0.10	1.27805	1.26371	1.20354	4.13123	4.07359	4.09317
			308.15 K			
0.00	1.05367	1.01968	0.97825	4.10432	4.06319	4.06586
0.02	1.08417	1.04734	1.00404	4.09158	4.05527	4.06070
0.04	1.11445	1.07558	1.03089	4.07694	4.04730	4.05544
0.06	1.14489	1.10342	1.05694	4.08595	4.05275	4.05885
0.08	1.17173	1.12611	1.07716	4.09606	4.05805	4.06216
0.10	1.18591	1.13817	1.08734	4.10241	4.06185	4.06487
			313.15 K			
0.00	0.98043	0.92181	0.86290	4.07834	4.05274	4.03684
0.02	1.00997	0.94877	0.88723	4.06599	4.04539	4.03215
0.04	1.03855	0.97543	0.91277	4.05376	4.03852	4.02752
0.06	1.06769	1.00287	0.93762	4.06440	4.04422	4.03068
0.08	1.09301	1.02409	0.95787	4.07306	4.04979	4.03440
0.10	1.10653	1.03521	0.96634	4.07942	4.05301	4.03652

shown in Figs 5-7. The variation of intermolecular free length and relaxation time are depicted in Figs 8-13 and the values are given in Table 3. Acoustic impedance has been shown in and Figs 14-16.

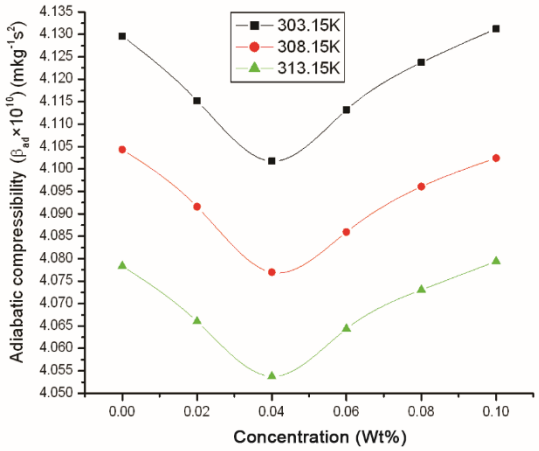

Fig. 5 – Plots of adiabatic compressibility of various nanofluids of CuO in 10% aqueous EG at different temperatures.

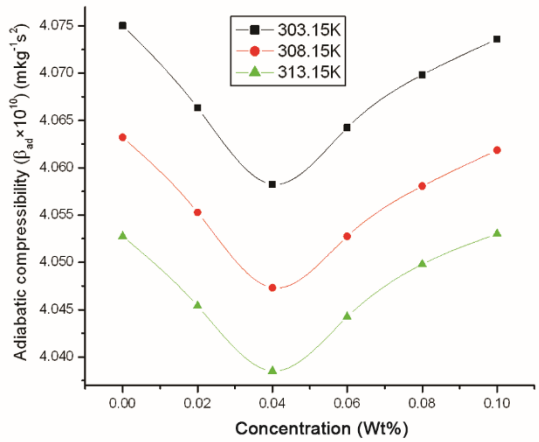

Fig. 6 – Plots of adiabatic compressibility of various nanofluids of CuO in 10% aqueous PG at different temperatures.

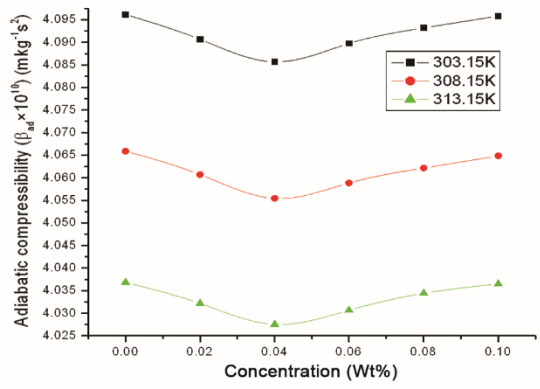

Fig. 7 – Plots of adiabatic compressibility of various nanofluids of CuO in 10% aqueous HG at different temperatures.

Acoustic impedance showed an increase with increase in concentration up to 0.04 wt% and beyond that concentration it showed a decrease. The increase in acoustic impedance at lower

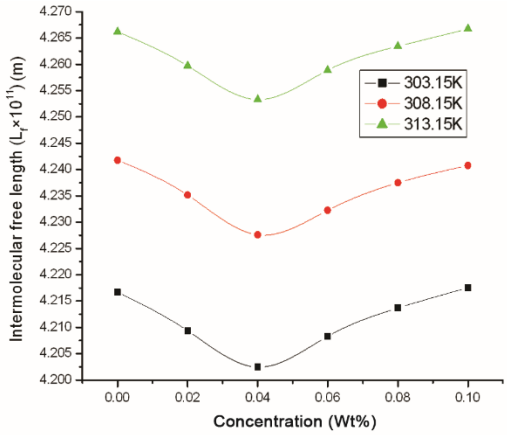

Fig. 8 – Plots of intermolecular free length of various nanofluids of CuO in 10% aqueous EG at different temperatures.

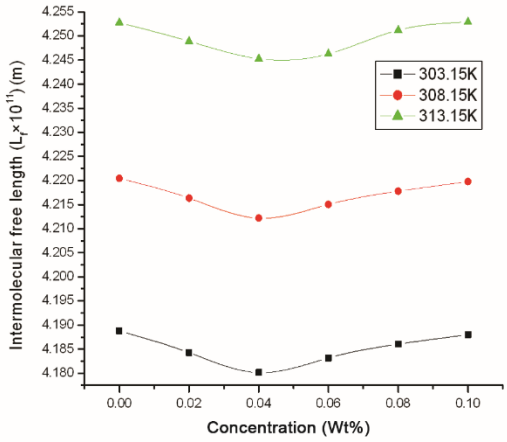

Fig. 9 – Plots of intermolecular free length of various nanofluids of CuO in 10% aqueous PG at different temperatures.

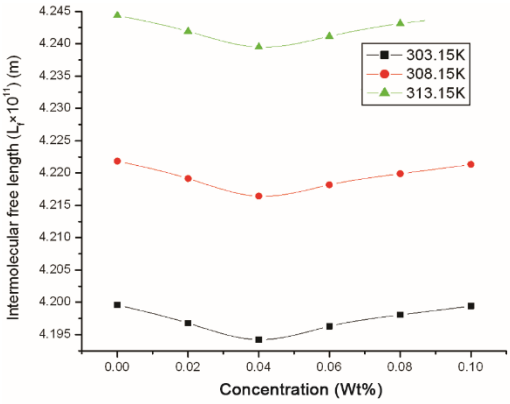

Fig. 10 – Plots of intermolecular free length of various nanofluids of CuO in 10% aqueous HG glycol at different temperatures.

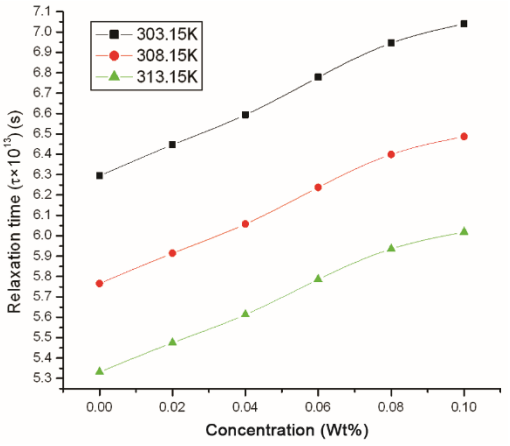

Fig. 11 – Plots of relaxation time of various nanofluids of CuO in 10% aqueous EG at different temperatures.

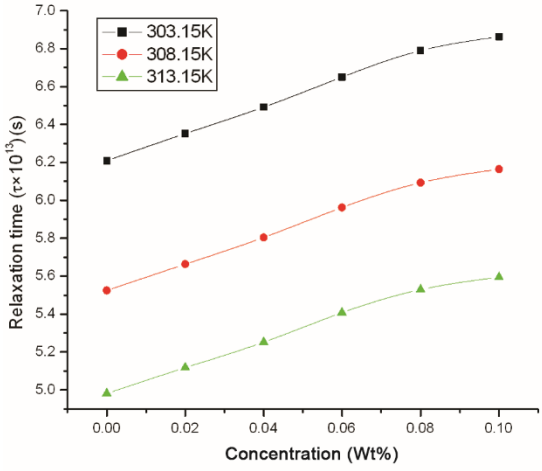

Fig. 12 –Plots of relaxation time of various nanofluids of CuO in 10% aqueous PG at different temperatures.

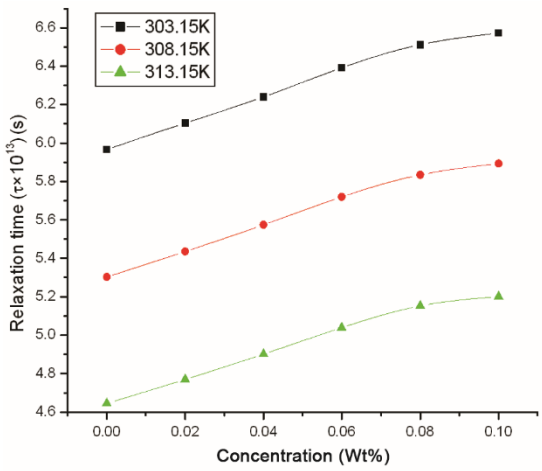

Fig. 13 – Plots of relaxation time of various nanofluids of CuO in 10% aqueous HG at different temperatures.

concentrations is due to increasing particle-fluid interactions and decrease at higher concentration is due to increasing particle-particle interactions. The increasing particle-fluid interactions at lower concentrations increases the intermolecular distance which creates the impedance in the propagation of ultrasonic waves. The increase in particle-fluid interactions at lower concentrations is also supported by a decrease in intermolecular free length. Attenuation coefficient showed an increase with increase in concentration of nanofluids as shown in Figs 17-19. With rise in temperature particle-fluid interactions showed an increase which is indicated by increase in ultrasonic velocity, acoustic impedance and intermolecular free length. Attenuation coefficient decreases with rise in temperature since the system become less dense and less viscous (Table 4). Relaxation time showed a decrease with rise in temperature because average kinetic energy of the particles increases with temperature.

It has also been observed that among three nanofluids the increasing order of particle-fluid interactions is HG < PG < EG indicated by the difference between successive values of ultrasonic velocity as shown in Table 1. At 303.15 K the difference between first two values of ultrasonic velocity in case of nanofluids of CuO with aqueous EG, aqueous PG and aqueous HG are 0.00236, 0.00147 and 0.00091, respectively. Similar results were also observed at different concentrations and at different temperatures. In all other parameters like ultrasonic velocity the difference between successive values is

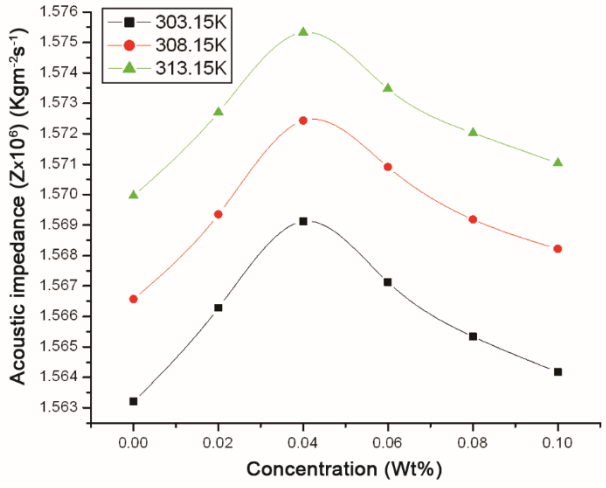

Fig. 14 – Plots of acoustic impedance of various nanofluids of CuO in 10% aqueous EG at different temperatures.

Table 3 — Intermolecular free length and relaxation time of CuO nanofluids at three different temperatures

Concentration (wt%)	$L_f \times 10^{11}$ (m)			$\tau \times 10^{13}$ (s)		
	EG+H_2O	PG+H_2O	HG+H_2O	EG+H_2O	PG+H_2O	HG+H_2O
			303.15 K			
0.00	4.21670	4.18874	4.19958	6.29439	6.20908	5.96640
0.02	4.20934	4.18426	4.19677	6.44640	6.35251	6.10375
0.04	4.20244	4.18011	4.19421	6.59420	6.49245	6.23977
0.06	4.20830	4.18319	4.19629	6.77770	6.65060	6.39165
0.08	4.21370	4.18606	4.19806	6.94540	6.78980	6.51224
0.10	4.21753	4.18800	4.19941	7.03989	6.86378	6.57265
			308.15 K			
0.00	4.24175	4.22045	4.22183	5.76613	5.52421	5.30324
0.02	4.23516	4.21633	4.21916	5.91462	5.66300	5.43615
0.04	4.22758	4.21219	4.21642	6.05806	5.80426	5.57429
0.06	4.23225	4.21504	4.21819	6.23729	5.96252	5.71995
0.08	4.23748	4.21778	4.21991	6.39931	6.09308	5.83412
0.10	4.24076	4.21975	4.22132	6.48678	6.16411	5.89319
			313.15 K			
0.00	4.26617	4.25276	4.24441	5.33137	4.98114	4.64452
0.02	4.25971	4.24890	4.24195	5.47538	5.11752	4.76993
0.04	4.25329	4.24529	4.23951	5.61338	5.25239	4.90160
0.06	4.25887	4.24628	4.24117	5.78603	5.40777	5.03899
0.08	4.26341	4.25121	4.24313	5.93586	5.52980	5.15258
0.10	4.26674	4.25290	4.24424	6.01866	5.59429	5.20087

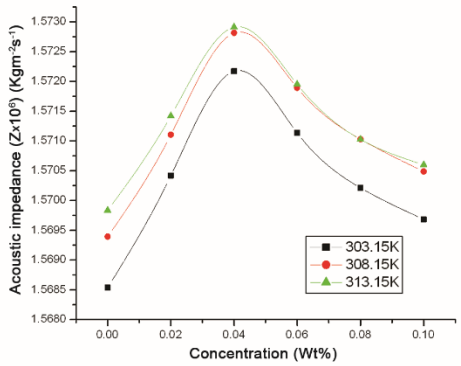

Fig. 15 – Plots of acoustic impedance of various nanofluids of CuO in 10% aqueous PG at different temperatures.

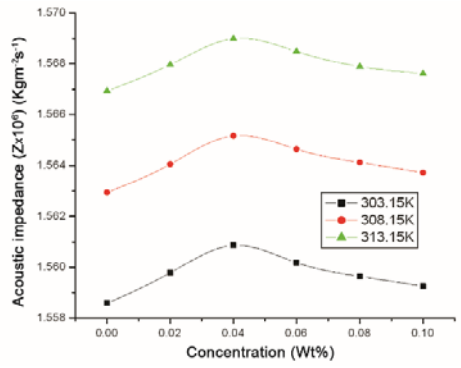

Fig. 16 – Plots of acoustic impedance of various nanofluids of CuO in 10% aqueous HG at different temperatures.

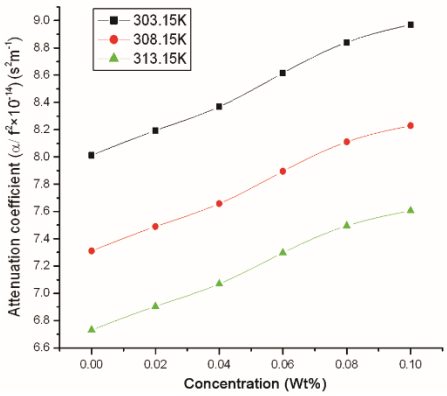

Fig. 17 – Plots of attenuation coefficient of various nanofluids of CuO in 10% aqueous EG at different temperatures.

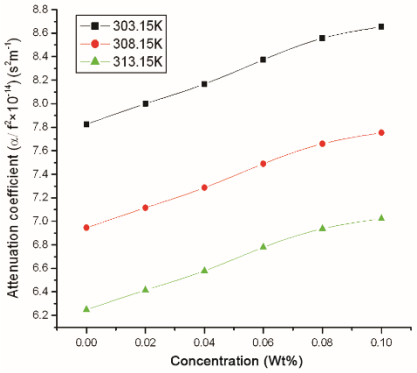

Fig. 18 – Plots of attenuation coefficient of various nanofluids of CuO in 10% aqueous PG at different temperatures.

Table 4 – Acoustic impedance and attenuation coefficient of CuO nanofluids at three different temperatures

Concentration (wt%)	$Z\times10^6$ (Kg m^{-2} s^{-1})			$\alpha/f^2\times10^{-14}$ (s^2 m^{-1})		
	EG+H_2O	PG+H_2O	HG+H_2O	EG+H_2O	PG+H_2O	HG+H_2O
			303.15 K			
0.00	1.56320	1.56854	1.55859	8.01247	7.82602	7.51122
0.02	1.56628	1.57042	1.55978	8.19348	7.99929	7.67967
0.04	1.56913	1.57217	1.56086	8.36905	8.16841	7.84669
0.06	1.56713	1.57113	1.56018	8.61496	8.37417	8.04215
0.08	1.56534	1.57021	1.55964	8.84066	8.55617	8.19791
0.10	1.56417	1.56968	1.55926	8.97055	8.65447	8.27733
			308.15 K			
0.00	1.56657	1.56939	1.56294	7.31081	6.94637	6.64546
0.02	1.56935	1.57110	1.56405	7.48906	7.11476	6.80820
0.04	1.57243	1.57282	1.56517	7.65824	7.28584	6.97717
0.06	1.57091	1.57189	1.56464	7.89458	7.49016	7.16304
0.08	1.56918	1.57103	1.56412	8.11078	7.65999	7.30955
0.10	1.56822	1.57049	1.56373	8.22932	7.75387	7.38666
			313.15 K			
0.00	1.56997	1.56984	1.56693	6.73136	6.24915	5.79326
0.02	1.57270	1.57142	1.56796	6.90425	6.41507	5.94667
0.04	1.57533	1.57291	1.56899	7.06878	6.57919	6.10778
0.06	1.57348	1.57195	1.56849	7.29671	6.77925	6.28192
0.08	1.57203	1.57103	1.56788	7.49468	6.93770	6.42697
0.10	1.57103	1.57060	1.56761	7.60629	7.02226	6.48946

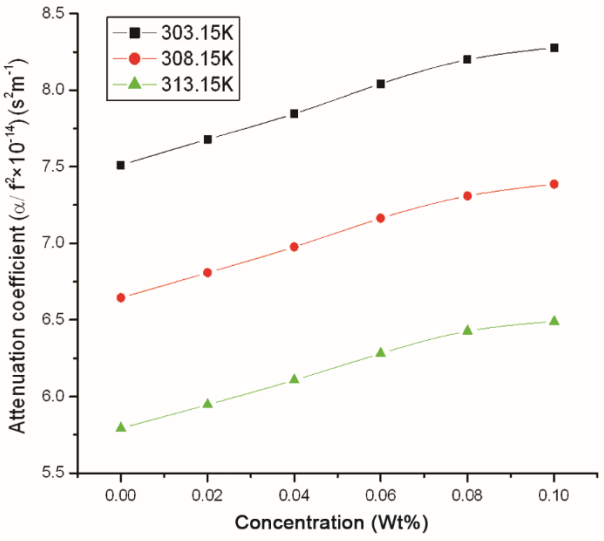

Fig. 19 – Plots of attenuation coefficient of various nanofluids of CuO in 10% aqueous HG at different temperatures.

HG < PG < EG which clearly shows that the particle-fluid interactions are maximum in case of nanofluids of CuO nanoparticles with aqueous EG and minimum in case of nanofluids of CuO nanoparticles with aqueous HG. This may be due to an increase in size of non polar part from EG to HG.

5 Conclusions

CuO nanoparticles were synthesised and characterized by XRD, TEM, SEM and EDX. With the help of ultrasonicator various nanofluids were obtained by dispersing the CuO nanoparticles in various base fluids. Various acoustical parameters were evaluated by using measured values of ultrasonic velocity, density and viscosity. The solute-solvent, solvent-solvent and solute-solute interactions were discussed in terms of these parameters as a function of concentration of CuO nanoparticles and temperature. From this discussion it has been concluded that concentration of CuO nanoparticles and temperature play important roles on the solute-solvent interactions. It has also been concluded that the chain length of the various glycols has an important effect on particle-fluid interactions. The interactions were maximum in nanofluids of CuO with aqueous EG and minimum in aqueous HG.

Acknowledgment

The authors are grateful to SAIF Cochin for providing XRD, SEM-EDX and TEM analysis facility and Department of Chemistry, University of Jammu for providing all other required facilities to carry out this work.

References

1 Choi S, *Enhancing thermal conductivity of fluids with nanoparticles,* in: Siginer D A & Wang H P (Eds), *Developments applications of non-newtonian flows*, (ASME: New York), 1995.
2 Chandrasekar M, Suresh S & Bose A C, *Exp Therm Fluid Sci*, 34 (2010) 210.
3 Lanje A S, Ningthoujam R S, Sharma S J, Pode R B & Vatsa R K, *Int J Nanotech*, 7 (2010) 979.
4 Jiang Y, Decker S, Mohs C & Klabunde K J, *J Catal*, 180 (1998) 24.
5 Larsson P O & Andersson A, *J Catal*, 179 (1998) 72.
6 Chikan V, Molnar A & Balazsik K, *J Catal*, 184 (1999) 134.
7 Poole C P, Datta T, Farach H A, Rigney M M & Sanders C R, *Copper oxide superconductors,* (John Wiley & Sons: New York), 1988.
8 Zabihi O & Ghasemlou S, *Int J Polym Anal Charact*, 17 (2012) 108.
9 Li Y, Wei Y, Shi G, Xian Y & Jin L, *Electroanalysis*, 23 (2011) 497.
10 Liu S, Tian J, Wang L, Qin X, Zhang Y, Luo Y, Asiri A M, Al-Youbi A O & Sun X, *Catal Sci Technol*, 2 (2012) 813.
11 Sundar L S & Sharma K V, *Int J Heat Mass Trans*, 53 (2010) 4280.
12 Zhou D, *Int J Heat Mass Trans*, 47 (2004) 3109.
13 Xuan Y & Li Q, *Int J Heat Fluid Flow*, 21 (2000) 58.
14 Jung J Y, Cho C, Lee W H & Kang Y T, *Int J Heat Mass Trans*, 54 (2011) 1728.
15 Lee S, Choi S U S, Li S & Eastman J, *J Heat Trans*, 121 (1999) 280.
16 Lee S & Choi S & Eastman J, *Trans ASME*, 121 (1999) 280.
17 Putnam S A, Cahill D G, Braun P V, Ge Z & Shimmin R G, *J Appl Phys*, 99 (2006) 084308.
18 Assael M, Chen C F, Metaxa I & Wakeham W, *Int J Thermophys*, 25 (2004) 971.
19 Xie H, Wang J, Xi T & Liu Y, *Int J Thermophys*, 23 (2002) 571.
20 Xie H, Lee H, Youn W & Choi M, *J Appl Phys*, 94 (2003) 4967.
21 Xue L, *Int J Heat Mass Trans*, 47 (2004) 4277.
22 Shaikh S, Lafdi K & Ponnappan R, *J Appl Phys*, 101 (2007) 064302.
23 Kang H, Kim S & Oh J, *Exp Heat Trans*, 19 (2006) 181.
24 Martin A & Bou-Ali M M, *CR Mec*, 339 (2011) 329.
25 Savithiri S, Pattamatta A & Das S K, *Nanoscale Res Lett*, 6 (2011) 471.
26 White S, Shih A & Pipe K, *Nanoscale Res Lett*, 6 (2011) 346.
27 Ijam A & Saidur R, *Appl Therm Eng*, 32 (2012) 76.
28 Yadav R R, Mishra G, Yadawa P K, Kor S K, Gupta A K, Raj B & Jayakumar T, *Ultrasonics*, 48 (2008) 591.
29 Tajik B, Abbassi A, Saffar-Avval M & Najafabadi M A, *Powder Technol*, 217 (2012) 171.
30 Karthikeyan N R, Philip J & Raj B, *Mater Chem Phys*, 109 (2008) 50.
31 Thirumaran S & Sudha S, *J Chem Pharm Res*, 2 (2010) 327.
32 Rowlinson J S & Swinton F L, *Liquid and liquid mixtures*, 3rd Edn. (Butterworths: London), 1982.
33 Povey M J W, *Ultrasonic techniques for fluids characterization*, (Academic Press: USA), 1997.
34 Morse P M & Ingard K U, *Theoretical acoustics*, (Princeton University Press: New Jersey), 1986.